TRANSPORT BARRIERS AND THE *q*-PROFILE

A.M.R. Schilham, M.R. de Baar, G.M.D. Hogeweij, N.J. Lopes Cardozo and the RTP team

FOM–Instituut voor Plasmafysica 'Rijnhuizen', Associatie Euratom–FOM,
Trilateral Euregio Cluster, P.O. Box 1207, 3430 BE Nieuwegein, The Netherlands

1. Introduction

In the Rijnhuizen Tokamak RTP ($R/a = 0.72/0.16$ m, $B_\phi < 2.5$ T, $I_\mathrm{p} < 150$ kA) experiments have been carried out combining the unique features of high power (5–10 times the Ohmic dissipation in the experiments shown), very localised ECH (2nd harm. X-mode) with high resolution T_e and n_e profile measurements. The experiments at hand are very detailed scans of the ECH deposition radius, r_dep. Figure 1 shows three examples. The T_e-profile, peaked for central ECH, becomes hollow for off-axis deposition [1,2]. The shape of the profile does not change smoothly variation of r_dep. Instead, the profile changes step-wise as exemplified by the central T_e as function of r_dep. Remarkably, the transitions are much sharper than the width of the power deposition. This striking experimental result was first published in [2] where it was pointed out that each transition is associated with the loss of a low order rational q value (1, 4/3, 3/2, 2, 5/2, 3,) from the q-profile, and that the difference between two T_e-profiles on either side of a transition was a narrow region of steep gradient, i.e. a transport barrier. In [2,3] the hypothesis is put forward that this phenomenology is caused by transport barriers near low-order rational q-values. A numerical implementation of this hypothesis proved capable of giving an excellent match to the experimental data. Independent corroboration for this hypothesis was found using modulated ECH, in particular in experiments on the so called 'non-local' central T_e rise [4].

Since the discovery of the phenomenon, the detailed r_dep-scans have been repeated for different plasma conditions, varying the electron density (line averaged density $\langle n_\mathrm{e} \rangle$) and the plasma current (I_p). In this paper we present three data sets, discuss the differences and similarities, and test the barrier hypothesis against all data.

2. The data sets

Detailed r_dep-scans were made for the following 3 sets of conditions:

Set I: I_p = 81 kA, $\langle n_\mathrm{e} \rangle$=3 $\times$ 10^{19} m^{-3}.
Set II: I_p = 65 kA, $\langle n_\mathrm{e} \rangle$=3 $\times$ 10^{19} m^{-3}.
Set III: I_p = 61 kA, $\langle n_\mathrm{e} \rangle$=1.5 $\times$ 10^{19} m^{-3}.

Typically a scan consists of > 50 discharges. Within a scan, $\langle n_\mathrm{e} \rangle$ is kept constant within 10%. Figure 1 shows the fingerprints of the 3 data sets: the central T_e as measured with Thomson scattering, as function of ρ_dep ($\rho = r/a$). All measurements are taken in a steady state phase of the plasma, > 100 energy confinement times and > 10 resistive skin times after ECH was switched on. The data presented here are scans of B_ϕ, keeping I_p fixed. The scans roughly cover the range $0 < \rho_\mathrm{dep} < 0.6$, with deposition on the low field side of the magnetic axis to achieve best localisation, minimizing effects of refraction. However, scans have been carried out for high field side resonance too, as well as vertical scans using a tiltable launching mirror. These

scans showed the same transitions, but were hampered by diffraction effects for $\rho_{\rm dep} > 0.3-0.4$, especially at high $n_{\rm e}$. The double sided scans were used to experimentally determine the relation between $\rho_{\rm dep}$ and B_ϕ.

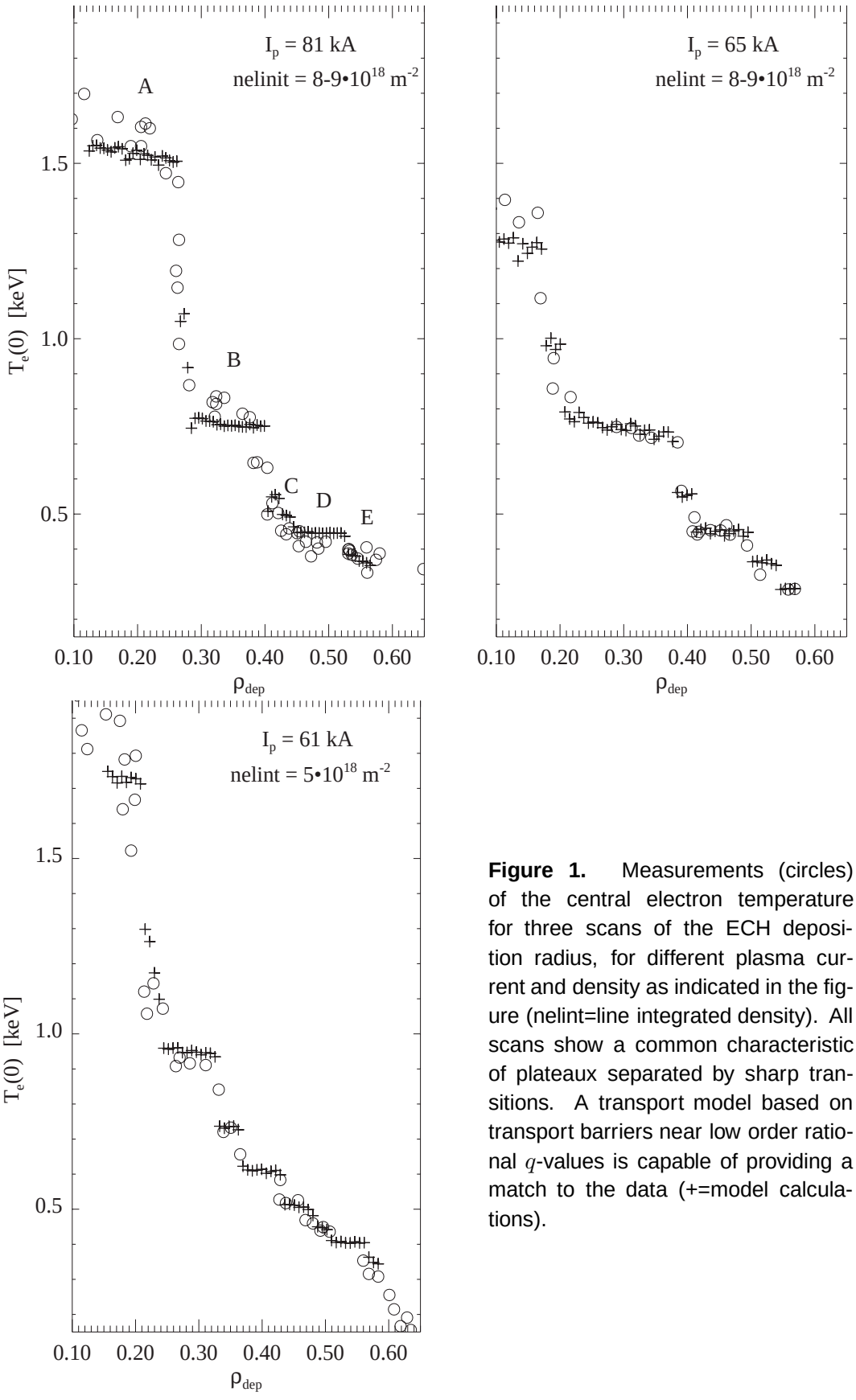

Figure 1. Measurements (circles) of the central electron temperature for three scans of the ECH deposition radius, for different plasma current and density as indicated in the figure (nelint=line integrated density). All scans show a common characteristic of plateaux separated by sharp transitions. A transport model based on transport barriers near low order rational q-values is capable of providing a match to the data (+=model calculations).

3. Phenomenological description

The most important observation is that all scans show the same sequence of plateaux and transitions. The sequence starts out with level A, which extends to $\rho_{\rm dep}$ =0.2–0.3. Inside level A the value of $\rho_{\rm dep}$ has little influence on $T_{\rm e}(0)$. Towards the end of level B the discharges are prone to $m = 2$ MHD activity, while very close to the B–C transition off-axis sawteeth are found [2,5,6]. Level C is relatively narrow, while near the D–E transition again off-axis sawteeth are found. The transition from level A to B passes through two sub-levels, in the lower of which again off-axis sawteeth are found, often with very long period.

Using the MHD behaviour to identify rational q-surfaces, as well as q-profiles calculated from the measured $T_{\rm e}$ and $n_{\rm e}$-profiles assuming neo-classical resistivity, the following systematic was found: level A: $q_{\rm min} < 1$; level B: $1.5 < q_{\rm min} < 2$; level C: $2 < q_{\rm min} < 2.5$, etc. [2,7]. Here $q_{\rm min}$ denotes the minimum value of q, which in cases of hollow $T_{\rm e}$-profiles often is assumed in an off-axis minimum.

The second important observation then is that also the systematic of the values of $q_{\rm min}$ for the sequences of plateaux is common to all three scans.

4. Analysis using a transport model with transport barriers

All data sets were analysed with the numerical transport model which features electron thermal transport barriers at (half)rational q-values (see Fig. 2), introduced and described in detail in [3]. It features an outward convective flux out to $\rho_{\rm dep}$, which is required to explain the hollow $T_{\rm e}$-

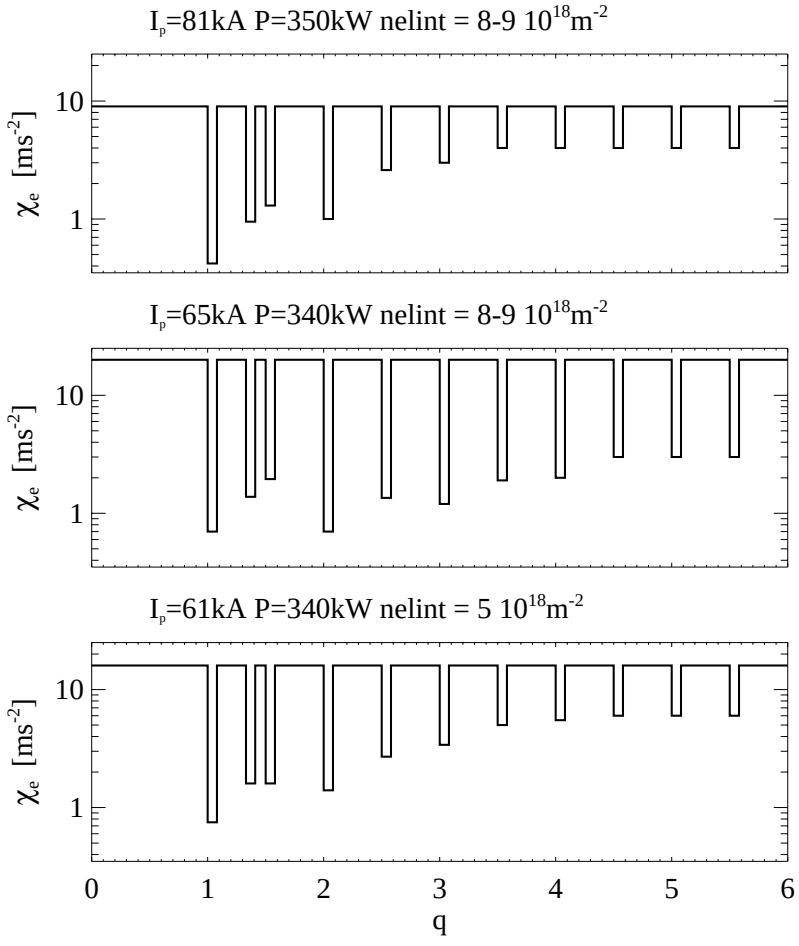

Figure 2. The transport model features transport barriers near low order rational q-values as indicated. Note that this model implies that the width of the barriers in real coordinates depends on the local shear. By varying the strength of the barriers and the value of $\chi_{\rm e}$ in the regions between the barriers, all three scans could be matched with essentially the same set of barriers.

profiles. The strength of this 'negative pinch' is kept constant for a scan. A single $\chi_{\rm e}(q)$ was used to model a $\rho_{\rm dep}$-scan at constant $I_{\rm p}$ and $n_{\rm e}$. The strength of the barriers was varied to get a match to the data, but the position of the barriers (expressed in a q-value) was kept the same for all scans. Since the heat resistance of a barrier is the ratio of its width and the local $\chi_{\rm e}$, the width (expressed in a q-range) of all barriers was taken equal. The behaviour of $T_{\rm e}(0)$ as function of $\rho_{\rm dep}$ was used as the principal measure for the quality of the match, but also the $T_{\rm e}$-profile shapes were used to constrain the model.

5. Results

1. For all scans, the model with transport barriers linked to q is capable of producing the basic features of the scans, i.e. the plateaux, the sharp transitions, as well as salient details of the $T_{\rm e}$-profiles such as the formation of sharp off-axis ears for deposition 'on top of' a transport barrier (not shown here).
2. The position of the barriers as function of q is kept the same for all scans. Thus, the differences in the values of $\rho_{\rm dep}$ for which transitions occur, come about through the different q-profiles.
3. From the scans with different $I_{\rm p}$ and different $n_{\rm e}$ we found:
- for constant density, the barriers are more pronounced at higher $q_{\rm a}$.
- for constant $q_{\rm a}$, the barriers are more pronounced at higher $\langle n_{\rm e}\rangle$.
- the 'turbulent' $\chi_{\rm e}$ in between the barriers is higher at higher $q_{\rm a}$.
- in all cases, the barrier near $q = 1$ is strongest; the barriers at higher q gradually become weaker.

6. Conclusions

The striking results of the ECH $\rho_{\rm dep}$-scan reported in [2] has now been reproduced in a number of plasma conditions, of which 3 cases have been presented in this paper. Data at other values of $I_{\rm p}$, $n_{\rm e}$ and the ECH power level have been acquired and are presently being analysed. The transport model with barriers at fixed q-values successfully describes the phenomenology. The barriers are most pronounced in high $q_{\rm a}$, high density discharges. The barriers have been shown to play an essential role in the non-local transport effects in RTP, as shown in [4].

Acknowledgement. This work was done under the Euratom–FOM association agreement, with financial support from NWO and Euratom.

References

[1] G.M.D. Hogeweij et al.: Phys. Rev. Lett **76** (1996) 632–635
[2] N.J. Lopes Cardozo et al.: Plasma Phys. Control Fusion **39** (1997) B303–316
[3] G.M.D. Hogeweij et al.: "A model for electron transport barriers in tokamaks, tested against experimental data from RTP." *Submitted to Nucl. Fusion*
[4] P. Galli et al.: *this conference*
[5] M. de Baar et al.: Phys. Rev. Lett **78** (1997) 4573-4576
[6] R.F.G. Meulenbroeks et al.: *this conference*
[7] F.A. Karelse et al.: *this conference*